LEGIBILITY NOTICE

LA-UR -90-650

MAR 0 5 1990

LA-UR--90-650

DE90 007497

TITLE FINITE ELEMENT MODELS TO PREDICT THE STRUCTURAL RESPONSE OF 120-mm SABOT/RODS DURING LAUNCH

AUTHOR(S) D. A. Rabern, K. A. Bannister

SUBMITTED TO U. S. Army Symp. on Gun Dynamics
Tamiment, PA
May 14-17, 1990

Los Alamos National Laboratory
Los Alamos, New Mexico 87545

TITLE: FINITE ELEMENT MODELS TO PREDICT THE STRUCTURAL RESPONSE OF 120-mm SABOT/RODS DURING LAUNCH

D. A. Rabern, Ph.D.*
Staff Member, Los Alamos National Laboratory
MS G787 Los Alamos, NM 87544

K. A. Bannister, Ph.D.
Staff Member, US Army Ballistic Research Laboratory
Aberdeen Proving Ground, MD 21005-5066

ABSTRACT:

Numerical modeling techniques in two- and three-dimensions were used to predict the structural and mechanical behavior of sabot/rod systems while inbore and just after muzzle exit. Three-dimensional transient numerical simulations were used to predict the rod deformations and states of stress and strain caused by axial and lateral accelerations during launch. The numerical models include the launch tube, recoil motion, and sabot/rod system modeled as it transits the launch tube and exits. The simulated rod leaves the muzzle of the gun, and exit parameters, including transverse displacement, transverse velocity, pitch, and pitch rate are extracted from the analysis results. Results from the inbore numerical simulations were compared with previous full-scale experiments. The results of the comparisons indicated a predictive capability to model inbore three-dimensional phenomena. Two-dimensional analyses were used to model details of the structural behavior caused by the axial load environment. Methodology and results are presented for several launch environments.

BIOGRAPHY:

PRESENT ASSIGNMENT:

Dr. Rabern's present responsibilities include the numerical and experimental design and evaluation of launch and terminal ballistic performance of kinetic energy munitions.

PAST EXPERIENCE:

Dr. Rabern worked for Thiokol Corporation for three years designing, modeling, and testing tactical rocket motors. He has worked for Los Alamos National Laboratory for the past six years performing dynamic structural and hydrodynamic calculations with supporting experiments to assess inbore and terminal effects of long rod penetrators and armored targets.

DEGREES HELD:

B. S. University of Utah 1979, Civil Engineering
M. S. University of Arizona 1983, Engineering Mechanics
Ph.D. University of Arizona 1988, Engineering Mechanics

FINITE ELEMENT MODELS TO PREDICT THE STRUCTURAL RESPONSE OF 120-MM SABOT/RODS DURING LAUNCH

D. A. Rabern, Ph.D.*
Los Alamos National Laboratory
Los Alamos, NM

K. A. Bannister, Ph.D.
US Army Ballistic Research Laboratory
Aberdeen Proving Grounds, MD

INTRODUCTION

Previous studies have used numerical simulations in two- and three-dimensions to characterize the structural response of sabot/rod systems during launch. Considerable effort was dedicated to axisymmetric finite element analyses to model the sabot and rod and their interface in quasi-static and dynamic simulations [1]. These calculations provide a good representation of stresses induced from the axial accelerations that occur during launch. They did not model the details of several sabot petals, tube straightness, or tube droop. More recent efforts have included using three-dimensional dynamic finite element analyses to model the axial and lateral accelerations associated with projectile launch from smooth-bore guns while the projectile was inbore [2,3]. This paper presents recent modeling techniques that extend numerical modeling capabilities in two- and three-dimensions to include inbore parameters that affect the flight path of the projectile. The analyses were focused on determining motions imparted to the projectile components during inbore travel and on understanding subsequent motions of the projectile after muzzle exit. The ultimate goals here are to ensure the structural integrity of the projectile during launch and to reduce the dispersion of kinetic energy (KE) rounds at the target. These recent code applications and methodologies are reviewed and typical results from the calculations are presented.

In sabot/rod systems the rod is very stiff in the axial direction and flexible in the lateral direction. A schematic of the M829 sabot/rod system is shown in Fig. 1. When subjected to lateral loads caused by the launch tube profile or by projectile balloting, the sabot/rod system vibrates. Artillery shells are stiff axially and laterally; vibrations in these systems contain higher frequency modes than

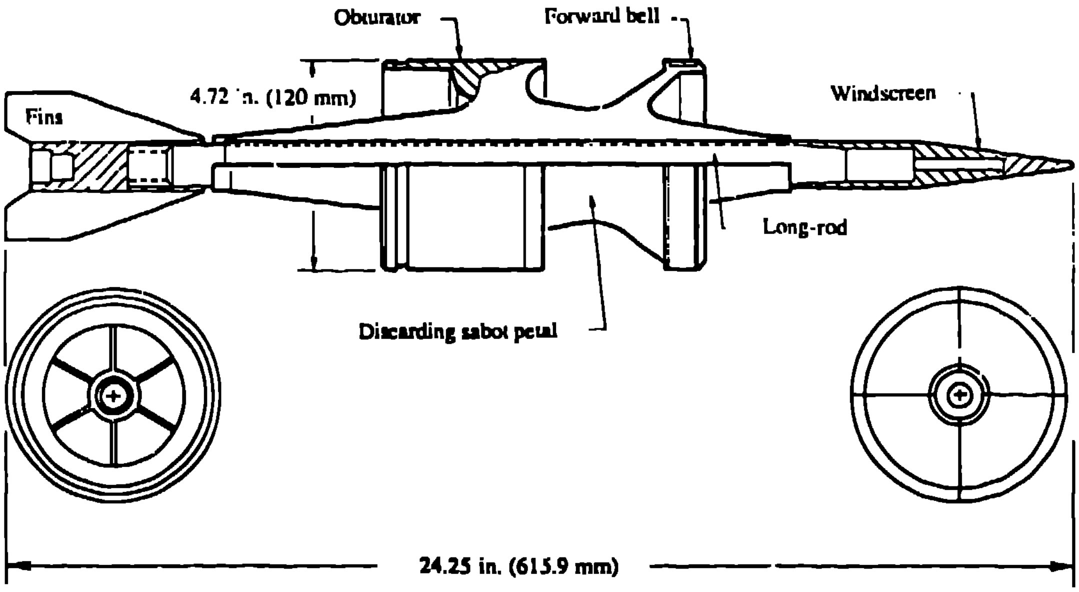

Figure 1. M829 sabot/rod schematic.

occur with the sabot/rod systems, but lateral bending is mimimal. A rough estimate of peak lateral accelerations for sabot/rod systems is 1 to 10% of the peak axial acceleration, or for the 120-mm gun, about 500 to 5000 g's. This lateral acceleration is the deciding criterion for determining whether two-dimensional axisymmetric analyses or three-dimensional analyses will suffice in a specific simulation. Three-dimensional analyses, while desirable, are expensive, and they require extensive computer resources. The advantage of two-dimensional models is that very detailed modeling of sabot/rod interfaces and system components can be completed. The disadvantages are the absence of the lateral or torsional load environments and the inability to model nonsymmetric geometry, such as the discontinuity associated with sabot petals.

Several numerical analysis approaches to model the launch of sabot/rod can be used, depending on the problem, the results needed, and the manpower and computer resources available to the analyst. Beam models for predicting the axial and lateral motion of the sabot and rod have been used with success for some applications. These codes usually run on personal computers that require minimal computing resources. Two-dimensional, finite element computations that are static and linearly elastic are used to study the axial load environment associated with launch. Two-dimensional dynamic, nonlinear analyses require additional computational resources, but they include important effects caused by the dynamic load environment and by material nonlinearity. Two-dimensional rezoning is also used to model materials with large nonlinear deformations, such as obturators, during the engraving process. Simulating the dynamic axial, lateral, and torsional environments with launch tube droop, eccentric masses, and nonsymmetric geometry requires dynamic three-dimensional finite element codes. These codes are used to model the gun and ammunition system for the duration of launch. A summary of the computational requirements for some typical inbore sabot/rod analyses is presented in Table I. This table is shown only to constrast the different analytical resources required.

TWO-DIMENSIONAL SIMULATIONS

A typical dynamic analysis of the M829 sabot/rod system in two dimensions was completed with the DYNA2D finite element code [4]. This type of analysis is used to determine the structural behavior of the sabot/rod system caused by the axial load environment. Changes in sabot geometry affect the way load is transferred to the rod. A two-dimensional dynamic analysis can be used to optimize sabot geometry to distribute the load into the rod as desired and mimimize the parasitic weight of the projectile.

TABLE I
COMPUTATIONAL RESOURCES FOR INBORE SIMULATIONS

Code Type	Problem Type	Approximate Computer Run Time (hours)	Code	Computer
2D-beam	Projectile + tube	0.5	RASCAL	Zenith PC
3D-beam	Projectile + tube	1-4	SHOGUN	Apollo WS
2D finite element	Projectile	1-2	DYNA2D	Cray XMP/48
2D finite element	Projectile + tube	6	DYNA2D	Cray XMP/48
2D finite element	Projectile + tube and 1D burn code	6-7	DYNA2D	Cray XMP/48
2D finite element	Projectile + tube + obturator (rezoning)	6-12	DYNA2D	Cray XMP/48
2D finite element	Projectile + tube + obturator (rezoning) and 1D burn code	8-13	DYNA2D	Cray XMP/48
3D finite element	Projectile + tube (180-deg course mesh)	7	DYNA3D	Cray XMP/416
3D finite element	Projectile + tube (360-deg medium mesh)	10-15	DYNA3D	Cray YMP

The finite element mesh of the sabot/rod are shown in the upper half of Fig. 2. The obturator is not shown in the figure. Details of the threaded interface were not considered in this analysis. Points A, B, and C are referenced to show typical stress results from a dynamic load environment. In the same figure, the axial stress for the three locations is plotted from propellant ignition to peak pressure. At location A the rod is being pulled and the corresponding tensile stress is indicated. At location B, near the center of the rod, compressive stress is indicated. Station C, near the front of the sabot, indicates a still higher compressive stress.

The long duration of load does not excite natural frequencies in this sabot/rod system. This indicates that a static analysis with peak pressure would be a reasonable compromise from which to determine stress levels in the sabot and rod when they are subjected to an axial load environment. If the load

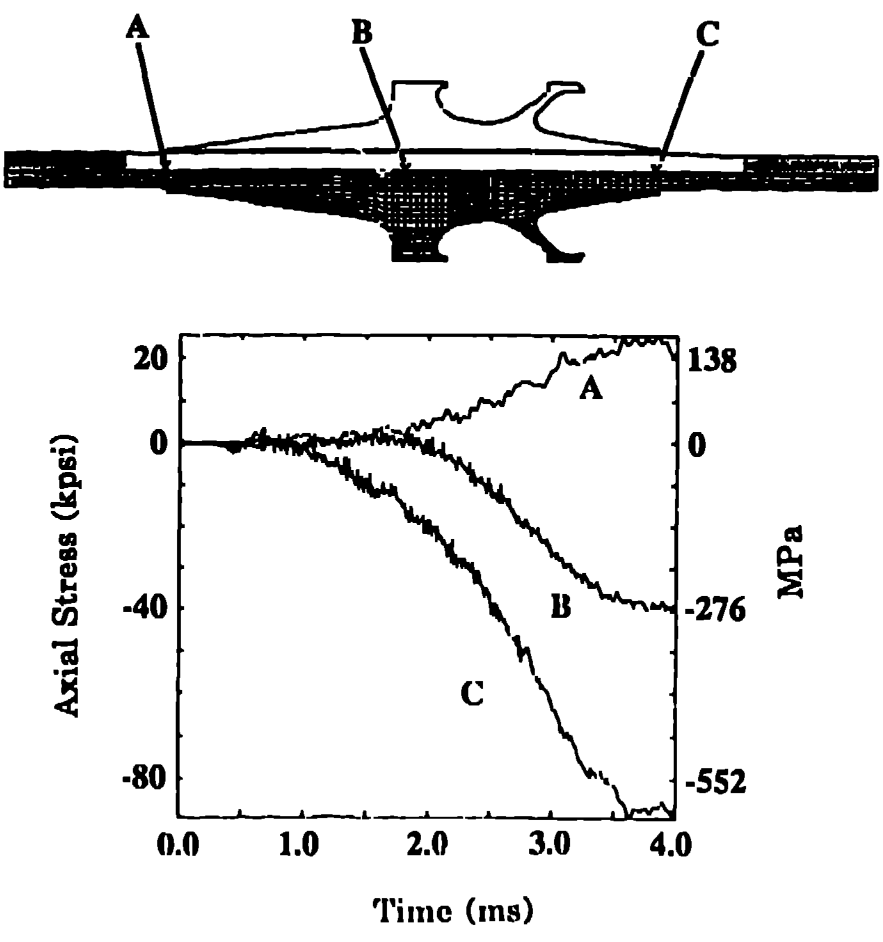

Figure 2. M829 two-dimensional finite element analysis.

duration occurs and causes natural frequencies to be excited during the launch process, a dynamic solution is required. Efforts to determine the natural frequency of the sabot/rod system are complicated by the shared boundary conditions between the sabot and rod and the sabot petal interfaces, and by the obturator and launch tube constraints. If natural frequency information is extracted numerically this will only provide data for the modeled system. Information from a finite element grid provides insufficient data to determine the actual natural frequency of a system, where the sabot can take compression, but no tension, in the hoop direction because of the sabot splits and because the sabot/rod interface takes shear loads but only mimimal radial loading.

Modeling of the threaded interface is best accomplished using a two-dimensional code. A good example of this type of modeling was documented by Costello [5]. Additional modeling areas include recent efforts to model the moving pressure front that follows the projectile in the launch tube and the coupled burn codes to predict the magnitude of the pressure, coupled with the mechanical and structural displacement of the projectile as it travels down the launch tube. These unpublished options are not widely implemented and are still in the research phase.

THREE-DIMENSIONAL SIMULATIONS

At the instant of firing, gun tubes are neither perfectly straight nor rigid, so the projectile travels along a flexible curved path. Each launch tube has a unique initial path that the projectile negotiates as it transits the tube. This path changes with tube motion because of recoil, breech block eccentricity, mounting conditions, and projectile, pressure, and propellent interactions. These issues must be considered before we can adequately predict the structural and mechanical performance of sabot/rod systems during launch. These components, as well as multiple sabot petals, require a three-dimensional analysis to predict lateral accelerations, tube movement, and tube/projectile interactions.

Previous work in three-dimensional analyses [2,3] were extended to include the projectile's behavior as it leaves the muzzle of the gun. Analyses and experiments were performed to establish a methodology for predicting the structural behavior of sabot/rod systems while inbore. The sabot/rod systems and their launch environments were modeled numerically to describe in detail the structural behavior of each system as it travels down each of the launch tubes. The numerical modeling was performed to predict the stress environment and the response of the sabot/rod system. The data obtained were used to compare the structural integrity of the three separate sabot designs in three separate launch environments. A brief description of the previous work performed is introduced here to explain how that work was enhanced to include near muzzle trajectory after exiting the launch tube.

Previous Work

The M829 sabot/rod (Fig. 1) was modeled in three different 120-mm smoothbore launch environments. The first launch tube was perfectly straight and was modeled to remove the effects of lateral loading on the sabot/rod system. The second launch tube, SN104, was used to observe the effect of minimal lateral loading on the sabot/rod system. The third launch tube, SN81, was used to observe the effects of significant lateral loads on the system. To obtain the initial launch tube profile of each tube, the launch tube was modeled with the ABAQUS [6] finite element code to determine the launch tube droop caused by gravity. Line-of-sight straightness data were superimposed on the tube droop to determine the initial launch tube profile before propellant ignition. Figure 3 presents the ABAQUS results (shown as the dashed line). The solid line represents the line-of-sight straightness for Launch Tube SN104. The addition of the lateral displacements associated with Lunch Tube droop and line-of-sight straightness provides the initial tube profile (shown as the dash-dot line). Figure 4 presents the same information for Launch Tube SN81. The two launch tube profiles are contrasted in Fig. 5. Launch Tube SN104 shows minimal deviation at the end of the launch tube. In Launch Tube SN81 the projectile must negotiate a significant launch path change in the high velocity sector of projectile launch.

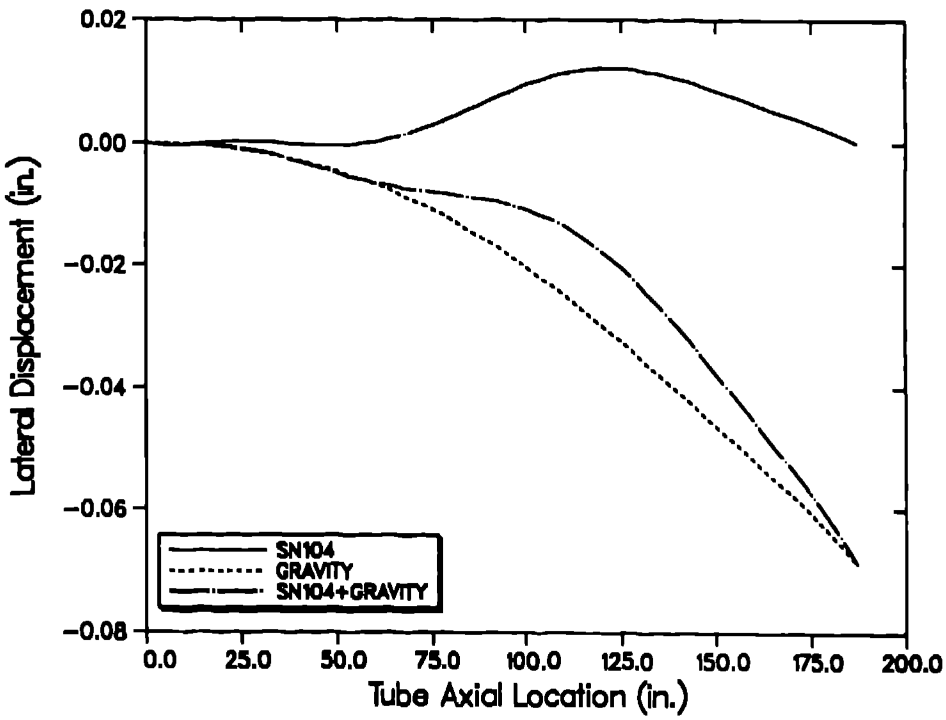

Figure 3. Lateral displacement versus axial location for Launch Tube SN104 at its initial state while under gravity loading and with the combination of the two.

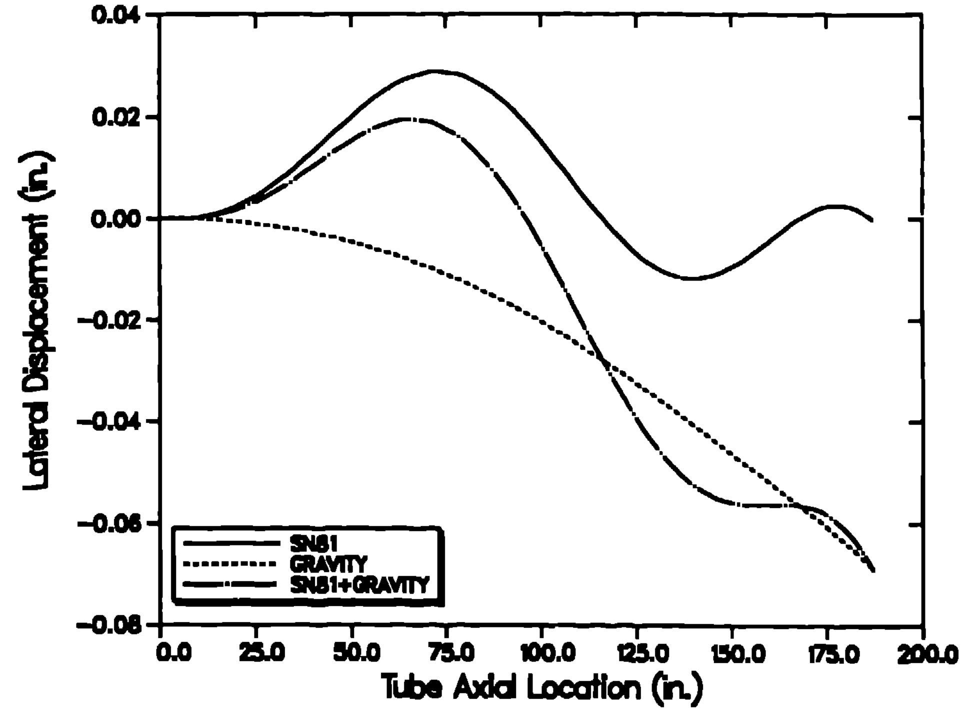

Figure 4. Lateral displacement versus axial location for Launch Tube SN81 at its initial state while under gravity loading and with the combination of the two.

These launch tubes were drawn from the US Army inventory. These profiles give an appreciation of the variability in straightness in a population of guns tubes and demonstrate the importance of considering this parameter in dynamic simulations of 120-mm gun systems. These particular launch tubes were choosen for the study for several reasons. Both launch tubes exhibit only small line-of-sight deviations parallel to the ground. This enables 180-deg three-dimensional analyses with a symmetry plane. With small changes in launch tube straightness parallel to the ground, high energy radiography equipment, which needs to be level, could be used to take radiographs of the sabot/rods through the launch tube and determine their deformed shapes caused by the launch tube lateral forcing function. Three launch environments and three M829 class sabot designs were studied numerically and experimentally to determine the launch environment and sabot design influence on inbore structural performance. The extended work presented in this paper addressed only the M829 sabot/rod in Launch Tubes SN81 and SN104.

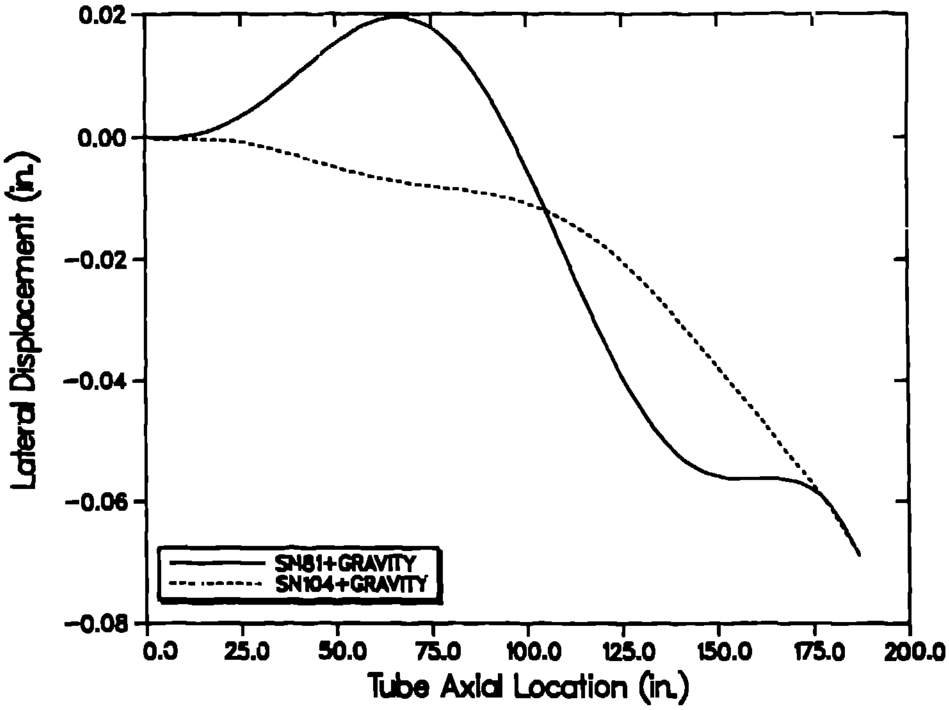

Figure 5. Comparison of lateral displacement versus axial location for Launch Tubes SN81 and SN104.

A full-scale test program was completed to determine the M829 rod deformed shape at three locations in Launch Tube SN81 and at two orthogonal stations after muzzle exit. Inbore radiography with a 2.3-MeV x-ray unit and orthogonal x-rays downrange were used to take radiographs of the sabot/rod in the launch tube and downrange [7]. Radiographs were digitized and processed to determine the centerline of the projectile at several locations inside and outside the launch tube. These data were used to benchmark numerical simulations completed earlier in the study.

DYNA3D [8], an explicit finite element code, was selected for the numerical analyses. This code has traditionally been used for dynamic transient analysis involving impact and contact surfaces. A 180-deg model, rather tnan a full 360-deg system, was generated. Appropriate boundary conditions were applied on the symmetry plane. The tube environment selected showed little motion normal to the constrained surface and was assessed to have small effects on the analysis results. With the 180-deg model, the problem size was cut significantly over a full 360-deg model. The M829 sabot/rod mesh in Launch Tube SN81 at time zero is shown in Fig. 6.

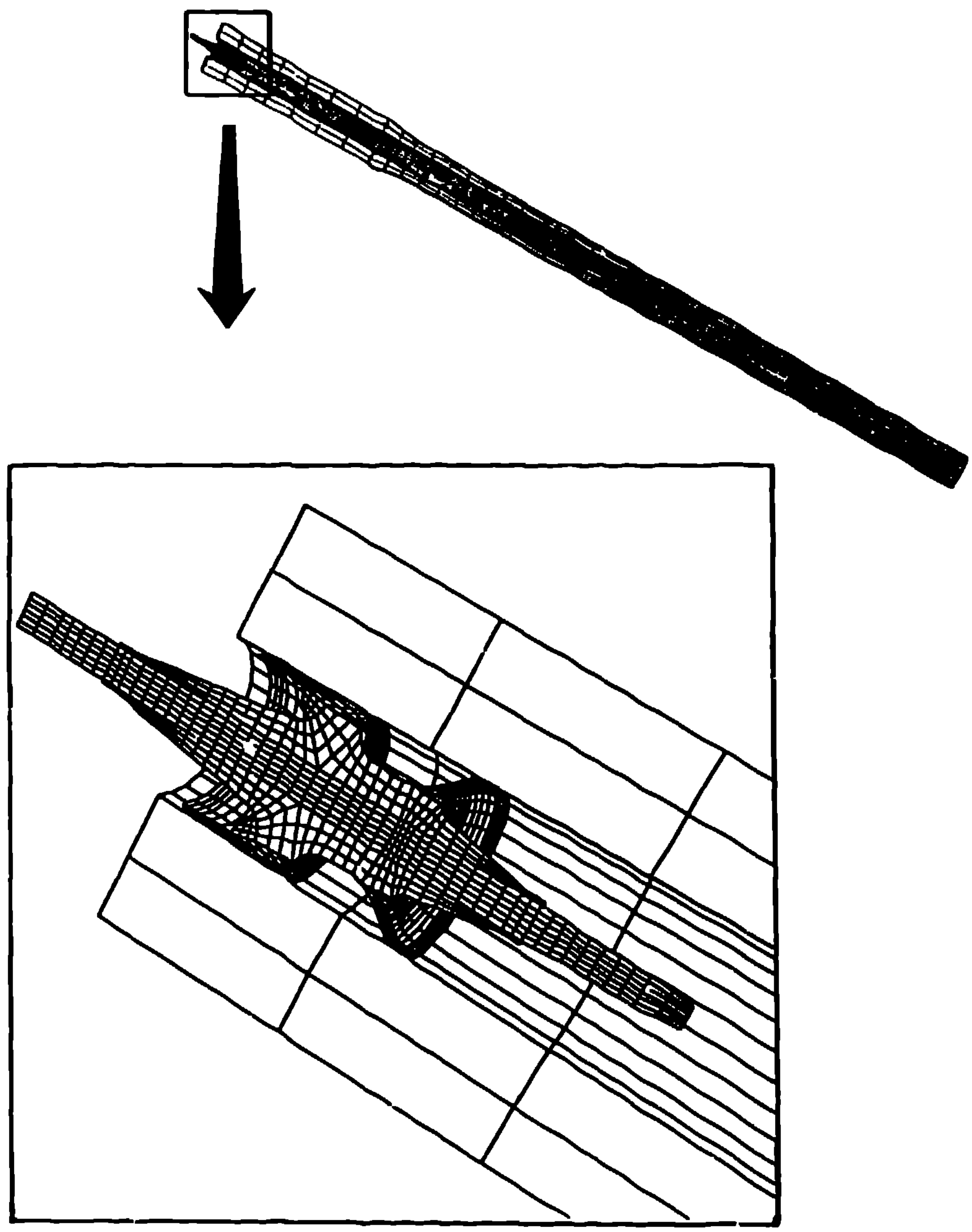

Figure 6. Finite element mesh of M829 sabot/rod system and launch tube.

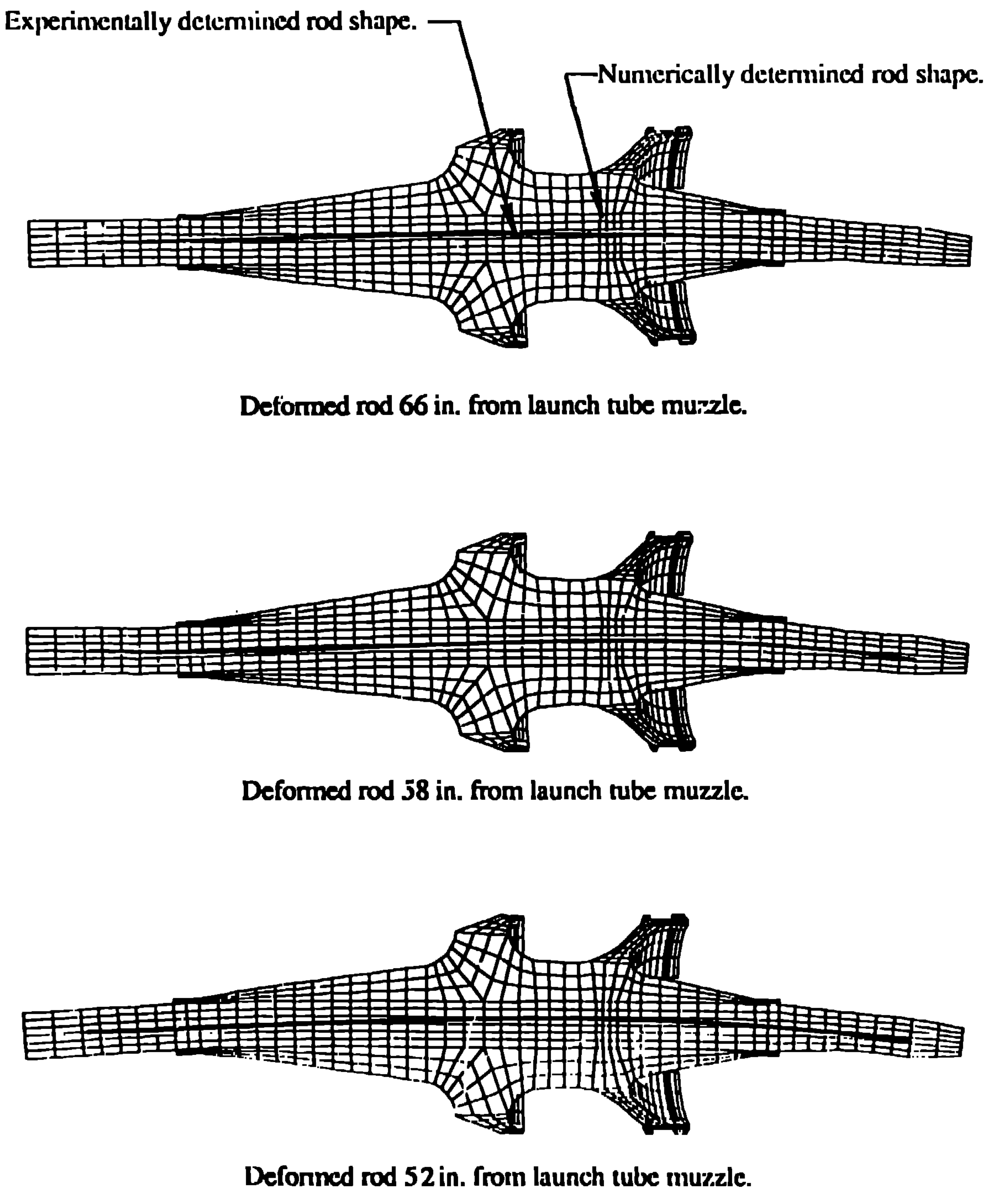

Figure 7. Comparison of numerically and experimentally determined rod deformed shapes.

The meshes consist of approximately 7000 nodes and 5000 eight-node hexahedron elements. Six materials, three sliding surfaces, two load curves, and approximately 1000 pressure surfaces are used in each model. Although each of the models differs slightly, the meshes are relatively similar. The fin, windscreen, and launch tube were modeled with elastic material models. The obturator, sabot, and rod were modeled with a work-hardening elastic-plastic material model. The sliding surfaces occur between sabot petals, between the obturator and the launch tube, and between the forward bell and the launch tube.

Results from three experiments were compared with results from the numerical analyses. In these tests the M829 sabot/rod was used in Launch Tube SN81. The deformed shape of the rod at the centerline was calculated for each test and was plotted at the same displacement scale factor as that used in the numerical analyses. These results are superimposed on the deformed finite element mesh at the corresponding axial locations in the launch tube. Shown in Fig. 7 are the comparisons at three separate locations. The launch tube's axial locations, rather than times, were chosen to account for the small differences in velocity between the physical testing and the numerical analyses. The numerical analyses were performed with an exit velocity of 1.65 km/s; the physical experiments showed velocities between 1.67 and 1.69 km/s. Axial locations were used to compare the results. As indicated in Figure 7 the deformed pattern from testing closely matches the numerical analyses. The top comparison shows the rod 66 in. from the launch tube muzzle. The measurement is made from the tail fins of the rod. The middle comparison shows the rod 58 in. from the muzzle, and the bottom comparison shows the rod 51 in. from the muzzle. These data show that the numerical analysis deformation cycle is slightly faster than shown in the physical tests. The effect is small. The general shape of both tests and numerical analyses agree well. Table II is a summary of the tip and tail displacements referenced from the center of gravity (c.g.) of the rod from both the numerical analyses and the physical tests.

Table III shows the peak von Mises stresses that occur in each launch environment at seven selected times during the launch process. The results indicate that for launch tube SN81, the lateral loadings do not significantly affect the sabot/rod until the velocity has increased in the latter stages of launch. At this point the effect, compared with the effect obtained using the perfectly straight (PS) launch tube, develops as much 296% higher stresses because of the lateral stress environment.

Extended Work

After the study was completed, questions arose concerning muzzle exit parameters. The M829 sabot/rod numerical models were modified to include the recoil motion of the launch tube. Originally, the numerical simulations were terminated at muzzle exit (7.2 ms). The M829 simulations in Launch Tubes SN81 and SN104 were rerun to 9.0 ms so data could be extracted beyond the muzzle.

TABLE II
COMPARISON OF TIP AND TAIL DISPLACEMENTS:
EXPERIMENTAL TESTING VS NUMERICAL ANALYSES
OF M829 IN LAUNCH TUBE SN81

Axial location from muzzle of gun (in.)	66	58	51
Numerical tip displacement (in.)	0.042	0.037	0.018
Experimental tip displacement (in.)	0.048	0.043	0.025
Numerical tail displacement (in.)	-0.016	0.004	0.032
Experimental tail displacement (in.)	-0.011	0.007	0.036

TABLE III
MAXIMUM VON MISES STRESS (ksi) FOR THREE LAUNCH ENVIRONMENTS
AT SEVEN SELECTED TIMES (s)

Time	0.0034	0.0039	0.0047	0.0053	0.0063	0.0069	0.0072
SN81	82	88	75	74	67	42	74
SN104	82	88	76	60	52	35	37
PS	82	88	76	63	37	29	25

The coordinate system for the calculations is the same as that used in the original M829 simulations. The coordinate system is shown in Fig. 8. The tube droop of the launch tube is 0.069 in. The angle between coordinate systems is 0.023° in the xy-plane.

The axial location of the sabot/rod is shown as a function of time in Fig. 9. The projectile exits the launch tube after 187 in. of travel. The simulation is terminated 293 in. from the projectile's orignal position or 106 in. after muzzle exit. Sabot separation and aerodynamic forces are not considered in these simulations. In reality, projectile motion will be influenced by sabot separation and aerodynamics. The axial velocity of the projectile is plotted in Fig. 10. The projectile accelerates to 5414 fps (1.65 km/s) until it exits at 7.2 ms. The velocity remains constant for the remainder of the simulation.

The average projectile lateral displacement presented in the numerical analysis coordinate system is shown in Fig. 11. The lateral displacement is calculated using several nodal traces along the axis of the rod and averaging these traces to determine the average lateral displacement of the rod for the M829 sabot/rod in Launch Tubes SN 81 and SN104. A positive lateral displacement

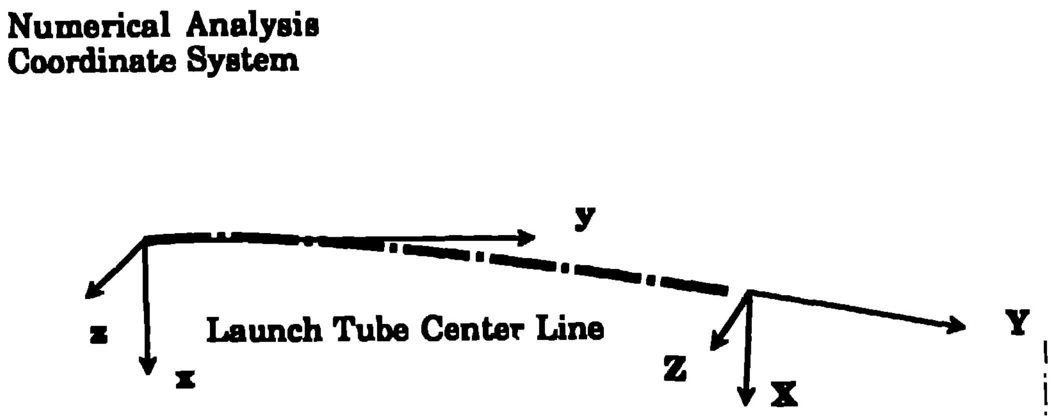

Figure 8. Analysis coordinate systems, M829 study.

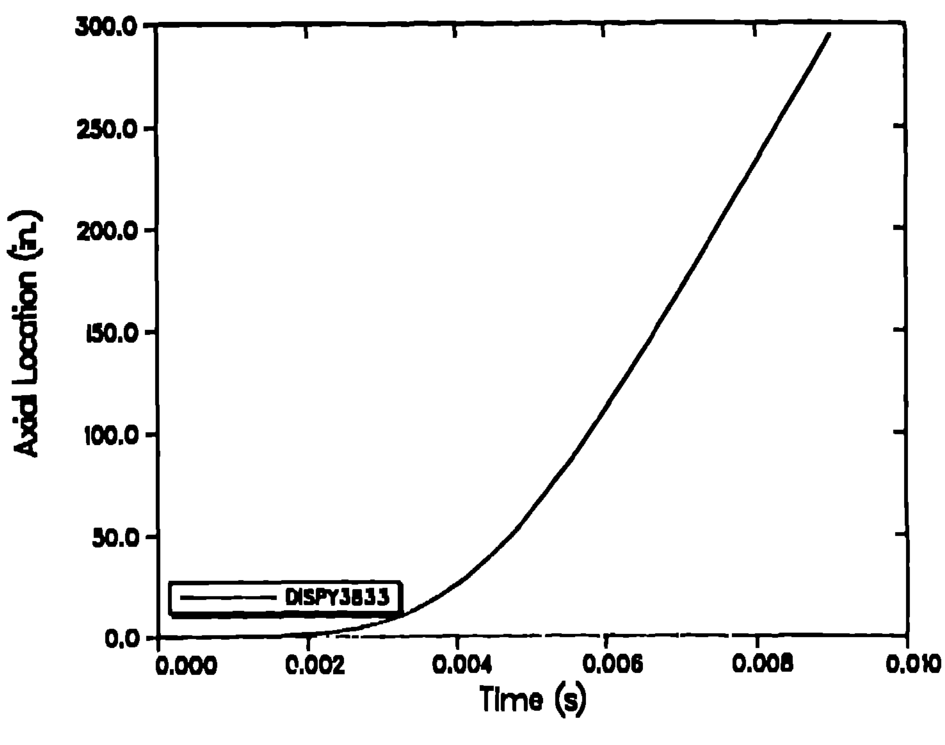

Figure 9. Axial location versus time for M829 sabot/rod.

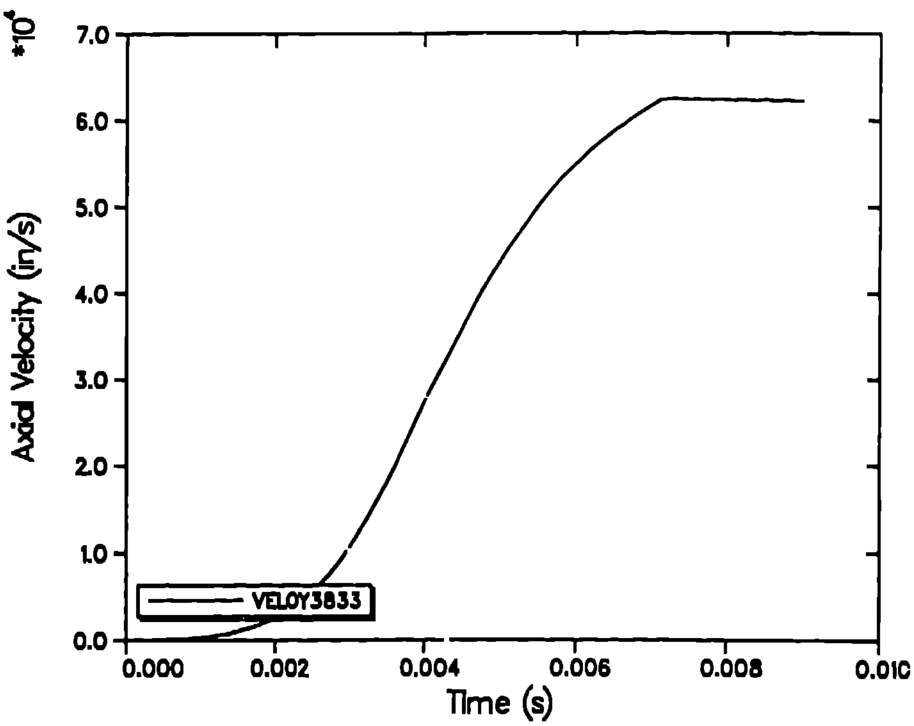

Figure 10. Axial velocity versus time for M829 sabot/rod.

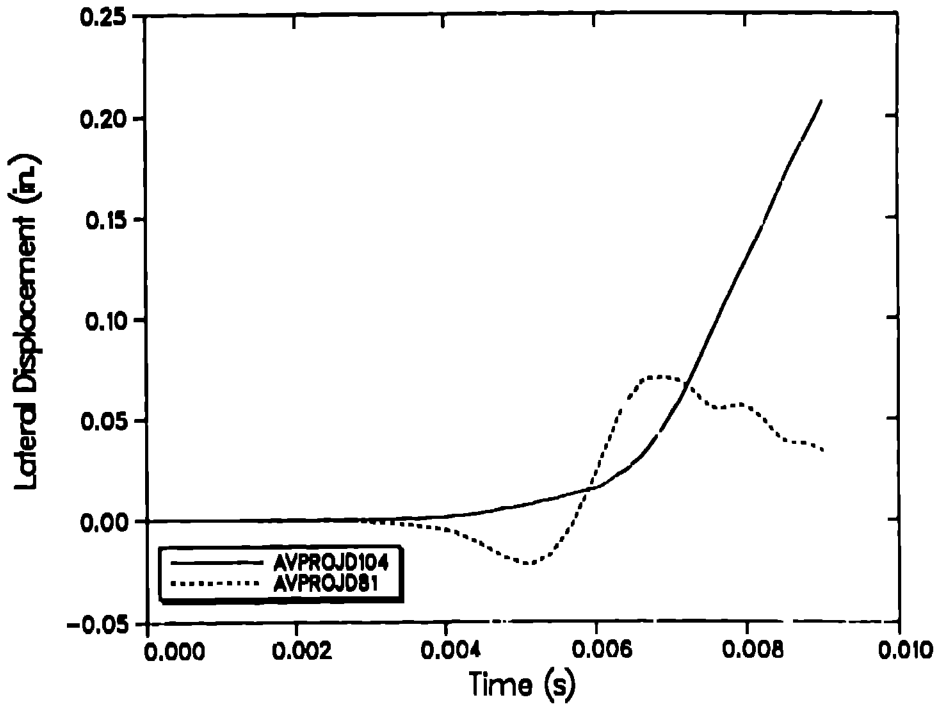

Figure 11. Average M829 projectile lateral displacement versus time for Launch Tubes SN81 and SN104.

indicates that the projectile is moving toward the ground. The lateral velocity for the two launch environments is shown in Fig. 12. This figure indicates that Launch Tube SN 81 causes an upward velocity of 23 in./s. Launch Tube SN104 produces a downward velocity of 76 in./s.

The tip and tail displacements referenced from the c.g. of the rod are shown for both launch tube environments in Fig. 13. The rigid body movement of the rod is removed by subtracting the lateral motion from the nodal traces at the tip and tail. The tip of the M829 sabot/rod in Launch Tube SN104 is plotted as the solid line, and the tail is plotted as the dashed line. The displacements are larger for Launch Tube SN81. The tip is shown as the dash-dot line and the tail as the dotted line.

The launch tube dynamics for the two cases considered are also plotted. Lateral displacement of the muzzle is shown for Launch Tube SN104 and SN81 in Fig. 14. The lateral velocity of the muzzle is shown in Fig. 15. A summary of the projectile and launch tube parameters at the muzzle exit are summarized in Table IV. The data presented are in the numerical analysis coordinate system (Fig. 8).

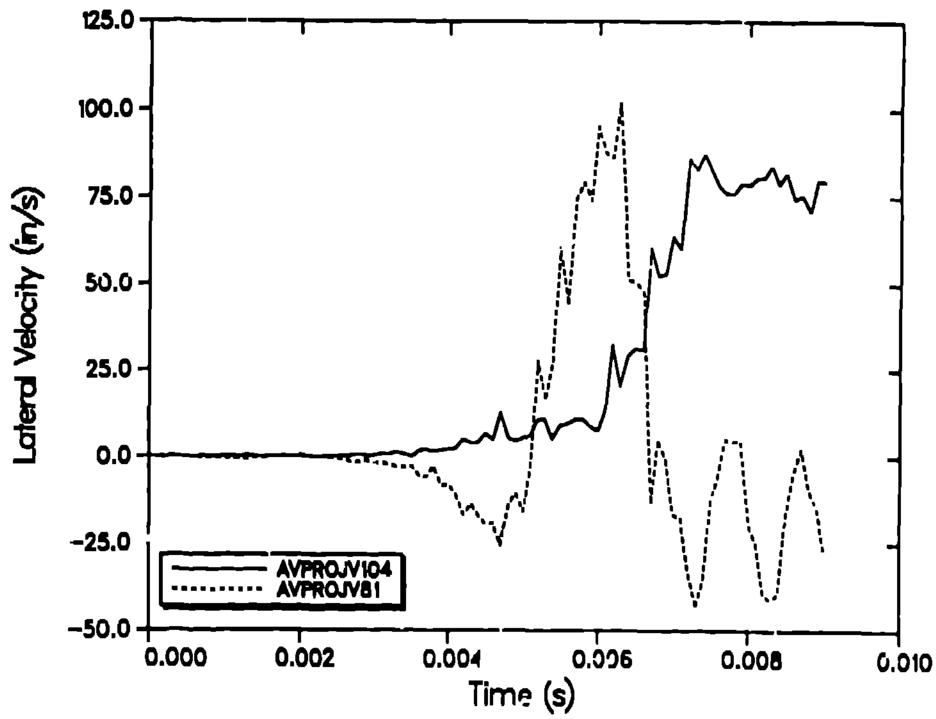

Figure 12. Average M829 projectile lateral velocity versus time for Launch Tubes SN81 and SN104.

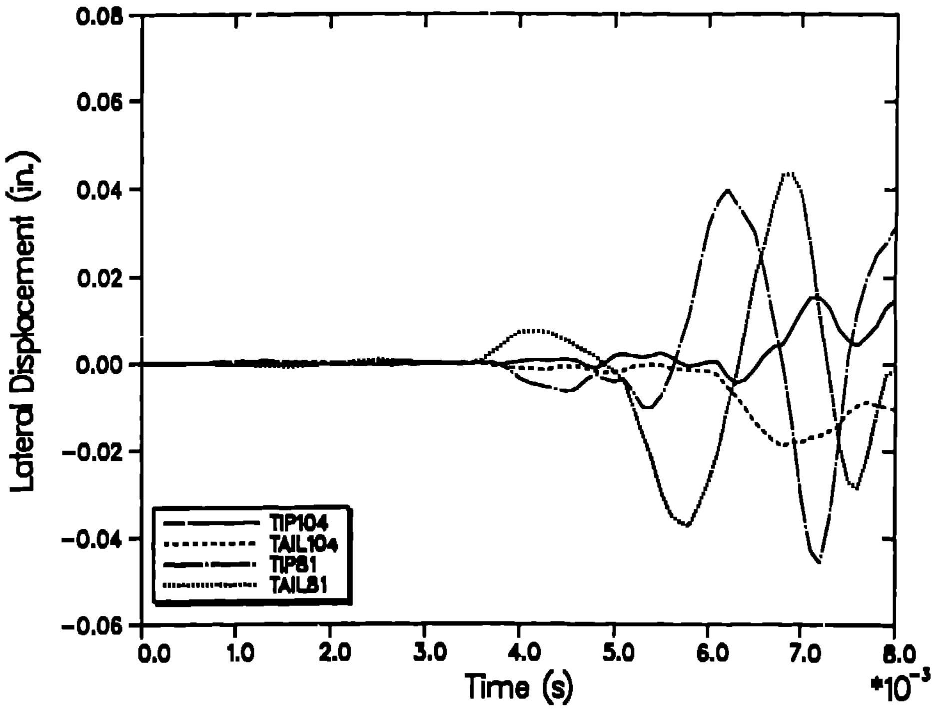

Figure 13. M829 tip and tail displacement with respect to the rod c.g. versus time in Launch Tubes SN81 and SN104.

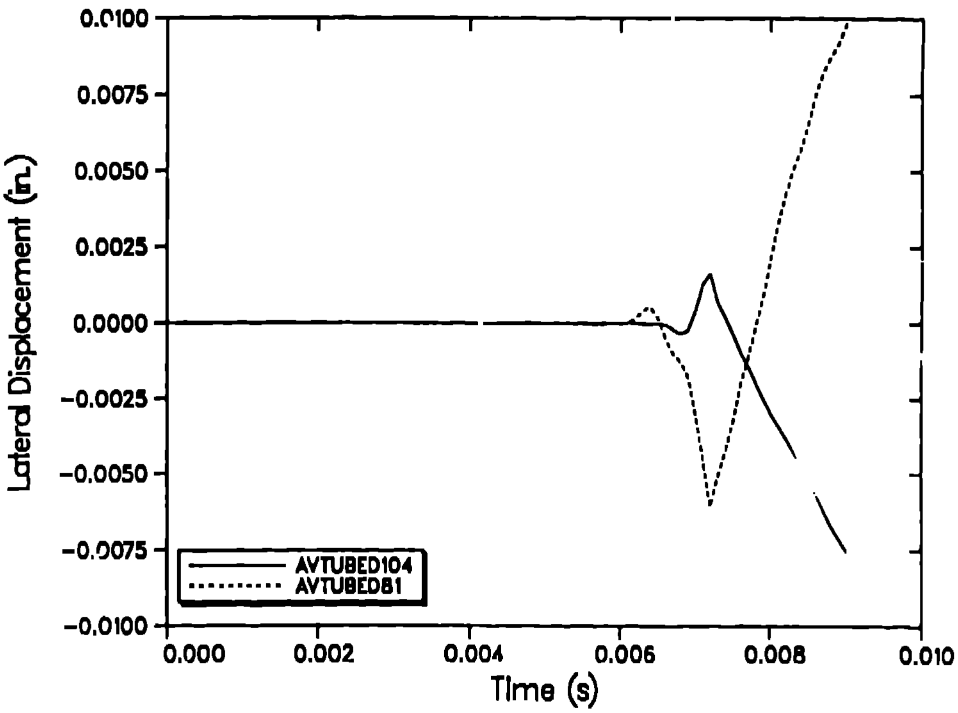

Figure 14. Average muzzle lateral displacement for Launch Tubes SN104 and SN81.

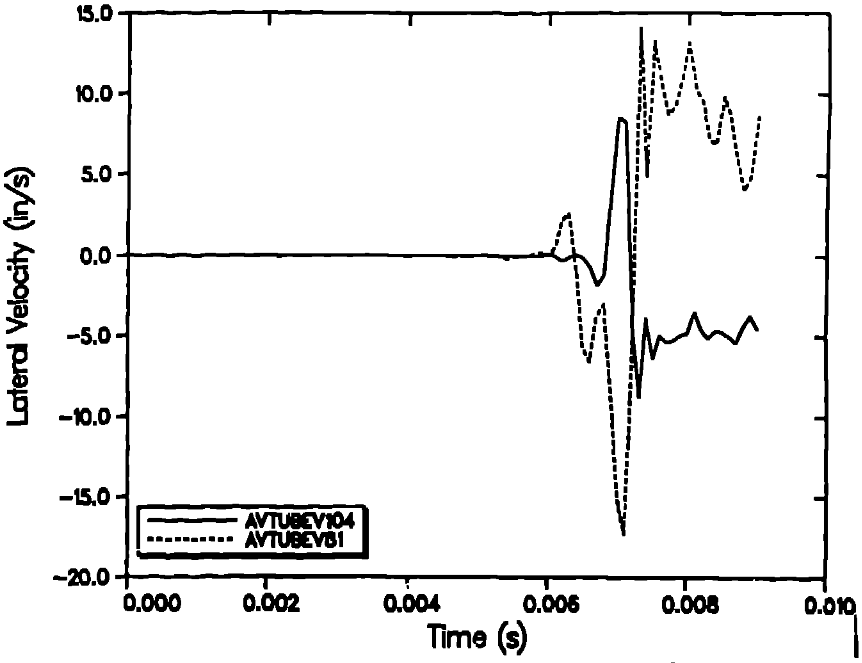

Figure 15. Average muzzle lateral velocity for Launch Tubes SN104 and SN81.

TABLE IV
DISPLACEMENT AND VELOCITY SUMMARY OF M829 SABOT/ROD LAUNCHED FROM LAUNCH TUBES SN81 AND SN104

Launch Environment	SN81	SN104
Projectile x displacement at exit (in.)	0.063	0.069
Projectile x-velocity at exit (in./s)	-23	77
Absolute maximum rod tip x-displacement with respect to rod c.g. (in.)	0.046	0.017
Absolute maximum rod tail x-displacement with respect to rod c.g. (in.)	0.042	0.019
Rod tip x-displacement with respect to rod c.g. at exit (in.)	-0.021	0.016
Rod tail x-displacement with respect to rod c.g. at exit (in.)	0.008	-0.007
Launch tube x-displacement at projectile exit (in.)	-0.006	0.001
Launch tube x-velocity at projectile exit (in./s)	7	-5

Data presented in the tables and figures have been referenced to the xyz-coordinate system outlined in Fig. 8. Lateral velocities, pitch, and yaw are more meaningful when referenced from the launch tube's pointing angle XYZ-coordinate system. This pointing angle coordinate system was used in the experimental program. Table V presents data from the both of the launch environments in the XYZ-coordinate system for lateral velocities, pitch, yaw, pitch rate, and yaw rate. Pitch and yaw data were taken 36 in. after muzzle exit. Data from Table V indicate that the projectile from Launch Tube SN81 flew upward with a lateral velocity of 49 in./s, with a downward pitch of 0.14 deg, rotating upward at a rate of 304 deg/s. The projectile from Launch Tube SN104 moved laterally down at 51 in./s, with a downward pitch angle of 0.05° and an upward rotation of 39 deg/s. Figure 16 is a schematic of projectile motion from each launch environment.

CONCLUSIONS

Numerical tools for predicting the structural and mechanical performance of sabot/rods during launch have been used in various applications. The results have been compared with experimental data to verify their validity. Modeling techniques have evolved to include the three-dimensional analyses of sabot/rods and gun systems.

TABLE V
MUZZLE EXIT PARAMETERS IN MUZZLE POINTING ANGLE COORDINATE SYSTEM FOR THE M829 SABOT ROD IN LAUNCH TUBES SN81 AND SN104

Launch Environment	SN81	SN104
Projectile X-velocity (in./s)	49 up	51 down
Projectile pitch 36 in. from muzzle (deg)	0.14 down	0.05 down
Pitch rate 36 in. from muzzle (deg/s)	304 up	39 up

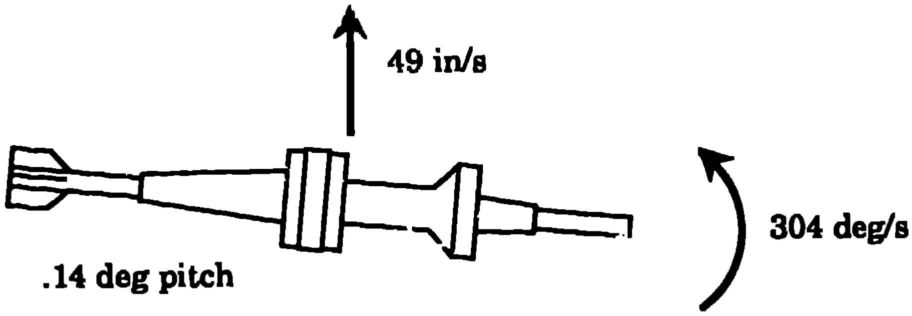

M829 36 in. from muzzle of launch tube SN 81

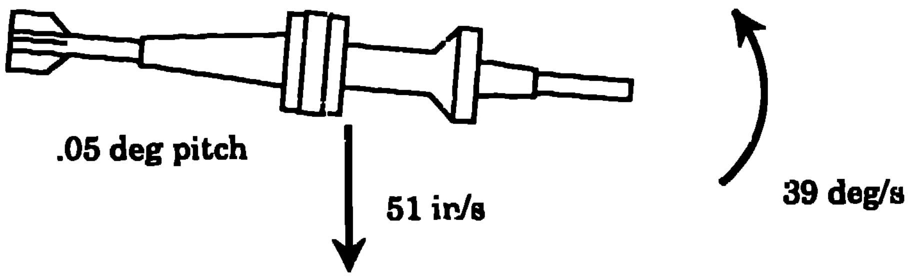

M829 36 in. from muzzle of launch tube SN 104

Figure 16. M829 sabot/rod motion, 36 in. after muzzle exit.

Two-dimensional finite element codes predict the axial performance of sabot/rod systems very well. Because peak pressure occurs early in projectile travel, the lateral load environment is small at this time. The projectile is moving slowly at peak pressure and has traveled only a short distance. Predicting the structural performance of the sabot/rod caused by lateral loads requires a three-dimensional analysis. The analyses needs to include seperate sabot petals, the launch tube and launch tube profile, and recoil. These analyses are well in hand but extensive postprocessing is required to make sense of the results. This is both time consuming and cumbersome, with large three-dimensional solutions. Careful evaluation of results is required to verify the validity of numerical models with complex geometry, dynamic load environments, sliding surfaces, nonlinear material response, and complex interfaces.

Future work in this area will provide more accurate solutions and greater capabilities for solving a wider class of problems. To accomplish this research in the area of sliding algorithms, code coupling with burn models and moving pressure fields are required. These efforts will enable the analyst to predict structural and mechanical behavior in gun and sabot/rod systems and will enable them to optimize their designs for lower parasitic weight of the sabot and mimimal dispersion caused by projectile launch.

ACKNOWLEDGMENTS

The United States Department of Army, Department of Energy and the Ballistic Research Laboratory funded this research. The authors wish to thank L. L. Shelley for editing this manuscript.

REFERENCES

1. Drysdale, W. H., "Design of Kinetic Energy Projectiles for Structural Integrity," U. S. Army Ballistic Research Laboratory technical report ARBRL-TR-02365, Aberdeen, Maryland (1981).
2. Rabern, D. A., "Axially Accelerated Saboted Rods Subjected to Lateral Forces," Los Alamos National Laboratory report LA-11494-MS, Los Alamos, New Mexico (1989).
3. Rabern, D. A., "In-bore Structural Behavior of 120-mm Saboted Long Rods Subjected to Axial and Lateral Accelerations," in *Proceedings of the 11th International Symposium on Ballistics*, Brussells, Belgium (1989).
4. Hallquist, J., O., "User's Manual for DYNA2D -- An Explicit Two-Dimensional Hydrodynamic Finite Element Code with Interactive Rezoning," Lawrence Livermore National Laboratory report UCID-18756, Rev. 2, Livermore, California (1984).
5. Costello, E. De L., "Computational Studies on the Launching of Long Rod Penetrators," *in Proceedings of the 11th International Symposium on Ballistics,* Brussells, Belgium (1989).
6. Hibbett, Karlson, and Sorenson Inc., *ABAQUS User's Manual Version 4.5a,* Providence, Rhode Island (1985).
7. Rabern, D. A., "Axially Accelerated Saboted Rods Subjected to Lateral Forces," *in Proceedings of the 1989 Flash Radiography Topical*, Welches, Oregon (1989).